

# Neutrino flavor transformation in supernova as a probe for nonstandard neutrino-scalar interactions

Yue Yang and James P. Kneller

*Department of Physics, North Carolina State University, Raleigh, NC 27695 USA\**

(Dated: November 2, 2018)

## Abstract

We explore the possibility of probing the nonstandard interactions between the neutrino and a hypothetical massive scalar or pseudoscalar via neutrino flavor transformation in supernovae. We find that in ultrarelativistic limit, the effective interaction between the neutrinos does not vanish if neutrinos are Majorana fermions but does vanish if neutrinos are Dirac fermions. The impact of the new neutrino interaction upon the flavor transformation above the neutrinosphere has been calculated in the context of the multi-angle “neutrino bulb model” and we find that the addition of the nonstandard neutrino self-interaction (NSSI) to the ordinary V-A self-interaction between neutrinos is capable of dramatically altering the collective oscillation when its strength is comparable to the standard, V-A, interaction. The effect of flavor-preserving (FP) NSSI is generally to suppress flavor transformation, while the flavor-violating (FV) components are found to promote flavor transformations. The neutrino signal from a Galactic supernova can provide complimentary constraints on scalar/pseudoscalar interactions of neutrinos as well as distinguishing whether the neutrino is a Majorana or Dirac fermion.

---

\* yyang30@ncsu.edu; jpknelle@ncsu.edu

## I. INTRODUCTION

The physical conditions found in the core of a core-collapse supernova (CCSN) provide us with an alternative and complimentary laboratory for probing the properties of the neutrino. In addition to the extreme matter density, the neutrino density in the vicinity of the proto-neutron star (PNS) is so high that neutrinos can experience coherent forward-scattering from the other neutrinos emitted from the PNS. Indeed, during some epochs of the explosion, this neutrino-neutrino self-interaction can dominate the flavor evolution. The complete description of the flavor transformation in CCSN is given in terms of Quantum Kinetic Equations [1–4] which are found to reduce to a Schrödinger-like equation in the limit where the exchange of energy and momentum vanishes. Using Standard Model physics, the Hamiltonian  $H$  that enters this equation is built out of a vacuum contribution  $H_V$ , a matter contribution  $H_M$ , and a self-interaction  $H_{SI}$ . The self-interaction makes the flavor evolution of one neutrino dependent upon the flavor evolution of every other neutrino it interacts with. The full problem is currently beyond the scope of computing platforms. The current state-of-the-art model for the calculations of neutrino flavor transformation in supernovae is known as the “neutrino bulb model” which imposes both spherical symmetry for neutrino emissions from the neutrinosphere, and axial symmetry around every radial ray, in order to reduce the number of independent variables needed to describe the neutrino field to just three. The three degrees of freedom are typically chosen to be: the radial coordinate along a ray, the neutrino energy, and the angle of emission relative to the normal at the neutrinosphere [5]. Multiple studies of the neutrino flavor transformation in CCSN have found the addition of  $H_{SI}$  can leave distinct features in the neutrino spectra which vary with time and which one would hope to observe in the signal from a future Galactic supernova: for recent reviews we refer the reader to Mirizzi *et al.* [6] and Horiuchi & Kneller [7]

The conditions found in a CCSN mean that any change to the properties of the neutrino often change the outcome of the flavor transformation. For example, new - sterile - flavors of neutrinos have been considered on several occasions [8–15]. Authors have found that active-sterile mass-splittings of order  $\sim 0.1 \text{ eV}^2$  or greater, and mixing angles larger than  $\sim 0.01^\circ$  can introduce new adiabatic Mikheyev-Smirnov-Wolfenstein (MSW) [16–18] resonances close to the PNS whose effect upon the neutrino flavor composition of the flux changes the dynamics of the explosion [12, 14] as well as the flavor evolution at larger radii and the

neutrino signal [12, 15].

Similarly one can also consider new interactions of neutrinos coupled via some new field to either matter (electrons and quarks) or to other neutrinos. There are several studies of the effect of nonstandard interactions of neutrinos with charged fermions and a pair of recent reviews can be found in Miranda and Nunokawa [19] and Ohlsson [20]. Again, these scenarios often lead to new resonances and flavor evolution which differs substantially from the Standard Model, V-A, case [21–29]. For example, it has been shown one can observe neutrino self-interaction effects in the normal mass ordering when nonstandard interactions are included that cannot occur with just Standard Model physics [26–29]. Alternatively one can also consider non-standard interactions of neutrinos among themselves - so-called non-standard self-interactions (NSSI). Compared with nonstandard interactions of neutrinos with charged fermions, the parameters of NSSI are much less constrained by terrestrial experiments [30–33] and current constraints show that NSSI can be as large as the standard neutrino self-interaction. This provides a unique opportunity for us to take advantage of the CCSN environments as a neutrino laboratory and place complimentary constraints upon unknown interactions among neutrinos.

The form of the NSSI is not unique. Recently Das et al. explored NSSI originating from a new gauge boson, which leads to an effective neutrino-neutrino interaction Hamiltonian similar to the standard V-A except for a flavor-dependent coupling strength and flavor-violating terms [34]. Their work was inspired by Blennow et al. [27] which used the same NSSI and was the first paper to put NSSI in the context of CCSN neutrino flavor transformation. These works show clearly that the presence of NSSI can have significant influence on neutrino flavor transformations. For example, it is pointed out the presence of NSSI can lead to flavor equilibration in both mass hierarchies [27], and it can also cause collective oscillation in normal mass hierarchy if NSSI is stronger than standard V-A [34].

While the gauge boson model is well-motivated, it only represents just one category of possible NSSI candidates. Another strong candidate for NSSI is a Yukawa coupling between neutrinos and nonstandard scalar or pseudoscalar fields. This type of interaction has a long history and is used in several models to explain the origin of neutrino mass. One prominent example is the “majoron model” by Gelmini [35, 36]. Constraints on the neutrino-majoron coupling by using the neutrino signal from SN1987A have been made [37–42] but these previous works did not link the neutrino-scalar coupling to neutrino flavor transformations

in supernovae.

Our goal in this paper is to explore the consequence of a neutrino-scalar/pseudoscalar interaction upon the flavor transformation. Our paper is organized in the following way. In section §II we write out the neutrino evolution equation and derive the single-particle effective Hamiltonian of NSSI under the mean field framework, showing the difference between what we derive with Dirac neutrino and Majorana neutrino. In section §III we solve the neutrino flavor evolution equations numerically with the NSSI term added to the standard Hamiltonian, using realistic supernova profiles and spectra, and show its impact on neutrino collective oscillations at two different time slices in the cooling phase of CCSN. We also make a comparison of the results by “single-angle” approach and “multi-angle” approach. In §IV we summarize our results and conclude.

## II. THE FLAVOR EVOLUTION OF SUPERNOVA NEUTRINOS

In this section we describe the formalism of neutrino flavor transformations in the supernova environment. During a supernova explosion, the ambient region around the contracting core is an environment featuring dense matter, violent turbulence, and an intense flux of neutrinos. What we want to compute is the flavor evolution history of these  $\sim 10^{58}$  neutrinos emitted as the PNS cools. As mentioned earlier, a full treatment of neutrino flavor evolution requires solving the quantum-kinetic equations taking all refraction and scattering effects into account. This is a gigantic task in terms of computational expense. Fortunately it has been demonstrated that neutrino flavor transformations usually happens in regions relatively far from the core due to the dense matter and multiangle suppression effect [43, 44], thus only the refraction effect is relevant and the Schrödinger-like flavor evolution equation for streaming neutrinos can be applied<sup>1</sup>.

---

<sup>1</sup> More recent works on “neutrino fast conversion” [45–48] indicate flavor transformations may occur close to the CCSN core potentially upsetting this paradigm.

### A. The equations of flavor evolution

The flavor evolution equation of a test neutrino propagating with momentum  $\mathbf{q}$  in the supernova environment takes the following form:

$$i \frac{dS_{\mathbf{q}}}{d\tau} = H(\tau, \mathbf{q}) S_{\mathbf{q}}, \quad (1)$$

where  $\tau$  is the “local proper time” [49] and  $S_{\mathbf{q}}$  is the matrix encoding the evolution history of the test neutrino. In ultrarelativistic and weak gravity limit, we can replace  $\tau$  with the distance  $r$  from the center of the neutrinosphere<sup>2</sup>. The probability that a neutrino in some generic initial state  $\nu_j$  with momentum  $\mathbf{q}$  at distance  $r_0$  is later detected as state  $\nu_i$  at distance  $r$  is  $P(\nu_j \rightarrow \nu_i) = P_{ij} = |S_{\mathbf{q};ij}(r; r_0)|^2$ . Similarly, the evolution of the antineutrinos can be given by an evolution matrix  $\bar{S}$  which evolves according to a Hamiltonian  $\bar{H}$ . The total Hamiltonian can be divided into three parts as

$$H(r, \mathbf{q}) = H_V(q) + H_M(r) + H_{\text{SI}}(r, \hat{\mathbf{q}}) \quad (2)$$

with  $\hat{\mathbf{q}}$  indicating a unit vector in the direction of the neutrino’s momentum. Note that the vacuum term  $H_V$  is only a function of neutrino energy, while the matter term  $H_M$  is only dependent on position  $r$ . The vacuum term and matter term are straight-forward to write out in the flavor basis for a relativistic three flavor neutrino with energy  $E$ :

$$H_V = \frac{1}{2E} U_V \begin{pmatrix} m_1^2 & 0 & 0 \\ 0 & m_2^2 & 0 \\ 0 & 0 & m_3^2 \end{pmatrix} U_V^\dagger, \quad H_M = \sqrt{2} G_F n_e(r) \begin{pmatrix} 1 & 0 & 0 \\ 0 & 0 & 0 \\ 0 & 0 & 0 \end{pmatrix}. \quad (3)$$

Under the standard model the self-interaction term in the Hamiltonian,  $H_{\text{SI}}$ , has a form which arises from the V-A interaction and is dependent on both the position and direction of the neutrino’s momentum. The expressions for self-interaction from the V-A interaction is

$$H_{V-A}(r, \hat{\mathbf{q}}) = \sqrt{2} G_F \int (1 - \hat{\mathbf{p}} \cdot \hat{\mathbf{q}}) [\rho(r, \mathbf{p}) dn_\nu(r, \mathbf{p}) - \bar{\rho}^*(r, \mathbf{p}) dn_{\bar{\nu}}(r, \mathbf{p})] dE. \quad (4)$$

where  $\rho(r, \mathbf{p})$  is the density matrix of the ambient neutrinos at position  $r$  with momentum  $\mathbf{p}$  and  $dn_\nu(r, \mathbf{p})$  is the differential neutrino number density [5], which is the differential contribution to the neutrino number density at  $r$  from those neutrinos with energy  $E = |\mathbf{p}|$

---

<sup>2</sup> Throughout the paper we set  $\hbar = c \equiv 1$ .

propagating in the directions between  $\hat{\mathbf{p}}$  and  $\hat{\mathbf{p}} + d\hat{\mathbf{p}}$ , per unit energy (the hats on  $\mathbf{p}$  and  $\mathbf{q}$  indicate unit vectors). The quantities  $\bar{\rho}(r, \mathbf{p})$  and  $dn_{\bar{\nu}}(r, \mathbf{p})$  are similar in meaning but for antineutrinos. The differential contribution  $\rho(r, \mathbf{p}) dn_{\nu}(r, \mathbf{p})$  can be further decomposed into  $\rho(r, \mathbf{p}) dn_{\nu}(r, \mathbf{p}) = \sum_{\alpha=e, \mu, \tau} \rho_{\alpha}(r, \mathbf{p}) dn_{\nu_{\alpha}}(r, \mathbf{p})$  by summing over the original flavor states of the neutrinos at the neutrinosphere.

## B. The effective Hamiltonian of NSSI

Let us consider the form of the additional contribution to  $H_{SI}$  from a hypothetical coupling between neutrinos via a scalar or pseudoscalar interaction. Instead of asking the nature of the hypothetical scalar fields, we focus on the phenomenological consequences if such a Yukawa coupling between neutrinos and some scalar fields exists. Generally the coupling can be written as

$$-\mathcal{L}_{\text{int}} = \frac{1}{2}g_{\alpha\beta}\bar{\nu}_{\alpha}\nu_{\beta}\phi + \frac{i}{2}h_{\alpha\beta}\bar{\nu}_{\alpha}\gamma^5\nu_{\beta}\chi, \quad (5)$$

where the  $\phi/\chi$  is the hypothetical scalar/pseudoscalar field, and  $\mathbf{g}$  and  $\mathbf{h}$  are the hermitian coupling matrices<sup>3</sup>. In many models the scalar fields are taken to be massless leading to new long range interactions, while in other models the scalar fields are massive shortening the range of the interaction considerably. The assumed mass and typical energy of the neutrinos have considerable impact upon the neutrino phenomenology. In this paper we assume the scalar(pseudoscalar) field has a mass larger than the GeV scale, which is well beyond the typical energies of supernova neutrinos. This excludes many scenarios in which the neutrino-scalar field coupling could change the CCSN dynamics through ‘‘cooling effects’’ [42]. This also makes it possible to adopt the ‘‘4-fermion’’ approximation, which is the basis of discussing neutrino-neutrino coherent forward scattering effect in the supernova environments. With this assumption, we can derive an effective neutrino NSSI Hamiltonian in addition to the regular V-A type neutrino self-interaction.

Under the assumption that the mediating particles  $\phi$  and  $\chi$  are sufficiently massive, the effective interaction Hamiltonian can be written in a 4-fermion form

$$\mathcal{H}_{\text{int}} = -\mathcal{L}_{\text{int}} \approx \frac{1}{8m_{\phi}^2}g_{\alpha\beta}g_{\xi\eta}(\bar{\nu}_{\alpha}\nu_{\beta})(\bar{\nu}_{\xi}\nu_{\eta}) - \frac{1}{8m_{\chi}^2}h_{\alpha\beta}h_{\xi\eta}(\bar{\nu}_{\alpha}\gamma^5\nu_{\beta})(\bar{\nu}_{\xi}\gamma^5\nu_{\eta}),$$

---

<sup>3</sup> For simplicity we assume  $\mathbf{g}$  and  $\mathbf{h}$  are real and symmetric in the following without loss of generality.

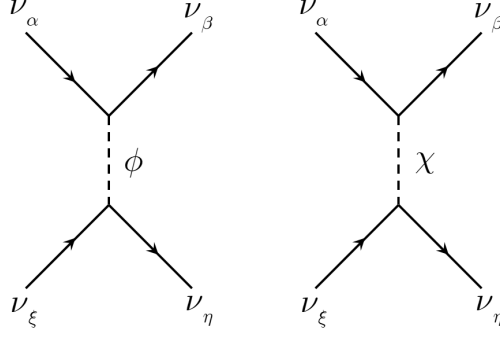


FIG. 1. The scalar and pseudoscalar interactions between neutrinos.

where  $m_\phi$  and  $m_\chi$  are the rest mass of  $\phi$  and  $\chi$ , respectively. Note that a factor of  $1/2$  has been introduced to avoid double counting. Just as with the V-A self-interaction, by applying the mean field approximation we can transform the 4-neutrino operators into an effective 2-neutrino operator (see appendix A). Interestingly, the resulting effective Hamiltonian holds different implications for Dirac neutrino and Majorana neutrino. For the Dirac neutrino we find

$$(\bar{\nu}_\alpha \nu_\beta) (\bar{\nu}_\xi \nu_\eta) \approx -\frac{1}{2} \langle \bar{\nu}_{\alpha L} \gamma^\mu \nu_{\eta L} \rangle (\bar{\nu}_{\xi R} \gamma_\mu \nu_{\beta R}) - \frac{1}{2} \langle \bar{\nu}_{\xi R} \gamma_\mu \nu_{\beta R} \rangle (\bar{\nu}_{\alpha L} \gamma^\mu \nu_{\eta L}) + (\alpha\eta \leftrightarrow \xi\beta) \quad (6)$$

and

$$(\bar{\nu}_\alpha \gamma^5 \nu_\beta) (\bar{\nu}_\xi \gamma^5 \nu_\eta) \approx \frac{1}{2} \langle \bar{\nu}_{\alpha L} \gamma^\mu \nu_{\eta L} \rangle (\bar{\nu}_{\xi R} \gamma_\mu \nu_{\beta R}) + \frac{1}{2} \langle \bar{\nu}_{\xi R} \gamma_\mu \nu_{\beta R} \rangle (\bar{\nu}_{\alpha L} \gamma^\mu \nu_{\eta L}) + (\alpha\eta \leftrightarrow \xi\beta) \quad (7)$$

where we have used  $(\alpha\eta \leftrightarrow \xi\beta)$  to denote the same terms with subscripts exchanged. Therefore, we have decomposed the scalar(pseudoscalar) coupling of neutrino fields into products of left-left coupling and right-right coupling of the vector-vector type. However, in the ultrarelativistic limit the right-handed component of neutrino fields vanishes, resulting in a zero contribution from right-handed neutrino current. So in the Dirac neutrino case, neither scalar nor pseudoscalar interactions can give us observable effects in the limit of vanishing neutrino mass.

But if neutrinos are Majorana fermions we find

$$(\bar{\nu}_\alpha \nu_\beta) (\bar{\nu}_\xi \nu_\eta) \approx -\frac{1}{2} \langle \bar{\nu}_{\alpha L} \gamma^\mu \nu_{\eta L} \rangle (\bar{\nu}_{\xi L}^C \gamma_\mu \nu_{\beta L}^C) - \frac{1}{2} \langle \bar{\nu}_{\xi L}^C \gamma_\mu \nu_{\beta L}^C \rangle (\bar{\nu}_{\alpha L} \gamma^\mu \nu_{\eta L}) + (\alpha\eta \leftrightarrow \xi\beta) \quad (8)$$

and

$$(\bar{\nu}_\alpha \gamma^5 \nu_\beta) (\bar{\nu}_\xi \gamma^5 \nu_\eta) \approx \frac{1}{2} \langle \bar{\nu}_{\alpha L} \gamma^\mu \nu_{\eta L} \rangle (\bar{\nu}_{\xi L}^C \gamma_\mu \nu_{\beta L}^C) + \frac{1}{2} \langle \bar{\nu}_{\xi L}^C \gamma_\mu \nu_{\beta L}^C \rangle (\bar{\nu}_{\alpha L} \gamma^\mu \nu_{\eta L}) + (\alpha\eta \leftrightarrow \xi\beta). \quad (9)$$

Unlike the Dirac neutrino, the charge conjugate currents of Majorana neutrino do not vanish even in the limit of zero neutrino mass. From the effective Hamiltonian operators (8) and (9) we can derive the single-particle Hamiltonian that can be used in neutrino flavor evolution equations by evaluating the average value of neutrino currents under single-particle states. In the following derivation we just consider a 2-flavor neutrino but from our result the generalization to neutrinos with more than 2 flavors is straightforward. The single-particle states for neutrino and antineutrino with momentum  $\mathbf{p}$  are

$$|\nu(\mathbf{p})\rangle = a_e |\nu_e(\mathbf{p})\rangle + a_x |\nu_x(\mathbf{p})\rangle, \quad |\bar{\nu}(\mathbf{p})\rangle = \bar{a}_e |\bar{\nu}_e(\mathbf{p})\rangle + \bar{a}_x |\bar{\nu}_x(\mathbf{p})\rangle. \quad (10)$$

Evaluating the average values on the single-particle states we obtain (see appendix A)

$$\langle \nu(\mathbf{p}) | \bar{\nu}_{\alpha L} \gamma^\mu \nu_{\beta L} | \nu(\mathbf{p}) \rangle = \frac{p^\mu}{E V} a_\alpha^* a_\beta, \quad \langle \bar{\nu}(\mathbf{p}) | \bar{\nu}_{\alpha L} \gamma^\mu \nu_{\beta L} | \bar{\nu}(\mathbf{p}) \rangle = -\frac{p^\mu}{E V} \bar{a}_\beta^* \bar{a}_\alpha \quad (11)$$

for normal currents and

$$\langle \nu(\mathbf{p}) | \bar{\nu}_{\alpha L}^C \gamma^\mu \nu_{\beta L}^C | \nu(\mathbf{p}) \rangle = -\frac{p^\mu}{E V} a_\beta^* a_\alpha, \quad \langle \bar{\nu}(\mathbf{p}) | \bar{\nu}_{\alpha L}^C \gamma^\mu \nu_{\beta L}^C | \bar{\nu}(\mathbf{p}) \rangle = \frac{p^\mu}{E V} \bar{a}_\alpha^* \bar{a}_\beta \quad (12)$$

for charge conjugate currents, respectively. Here  $p^\mu = (p, \mathbf{p})$  is the 4-momentum. If we define the single-particle density matrices as [5]

$$\rho(\mathbf{p}) = \begin{pmatrix} |a_e|^2 & a_e a_x^* \\ a_e^* a_x & |a_x|^2 \end{pmatrix}, \quad \bar{\rho}(\mathbf{p}) = \begin{pmatrix} |\bar{a}_e|^2 & \bar{a}_e \bar{a}_x^* \\ \bar{a}_e^* \bar{a}_x & |\bar{a}_x|^2 \end{pmatrix} \quad (13)$$

for neutrinos and antineutrinos respectively, then the final single-particle effective Hamiltonian of the non-standard neutrino self-interaction can be written as

$$H_S(r, \hat{\mathbf{q}}) = 4 \int (1 - \hat{\mathbf{p}} \cdot \hat{\mathbf{q}}) \{ \tilde{\mathbf{g}} [\rho^*(r, \mathbf{p}) dn_\nu(r, \mathbf{p}) - \bar{\rho}(r, \mathbf{p}) dn_{\bar{\nu}}(r, \mathbf{p})] \tilde{\mathbf{g}} \} dE \quad (14)$$

for neutrino-neutrino interaction via a scalar field and similarly,

$$H_P(r, \hat{\mathbf{q}}) = 4 \int (1 - \hat{\mathbf{p}} \cdot \hat{\mathbf{q}}) \{ \tilde{\mathbf{h}} [\rho^*(r, \mathbf{p}) dn_\nu(r, \mathbf{p}) - \bar{\rho}(r, \mathbf{p}) dn_{\bar{\nu}}(r, \mathbf{p})] \tilde{\mathbf{h}} \} dE \quad (15)$$

for neutrino-neutrino interaction through a pseudoscalar field. The elements of  $\tilde{\mathbf{g}}$  and  $\tilde{\mathbf{h}}$  are  $(\tilde{\mathbf{g}})_{\alpha\beta} \equiv \tilde{g}_{\alpha\beta} = \frac{1}{4m_\phi} g_{\alpha\beta}$  and  $(\tilde{\mathbf{h}})_{\alpha\beta} \equiv \tilde{h}_{\alpha\beta} = \frac{1}{4m_\chi} h_{\alpha\beta}$ . Note that equations (14) and (15) are valid for a neutrino model with arbitrary number of flavors.

### III. THE EFFECTS OF NSSI ON NEUTRINO FLAVOR TRANSFORMATION IN SUPERNOVAE



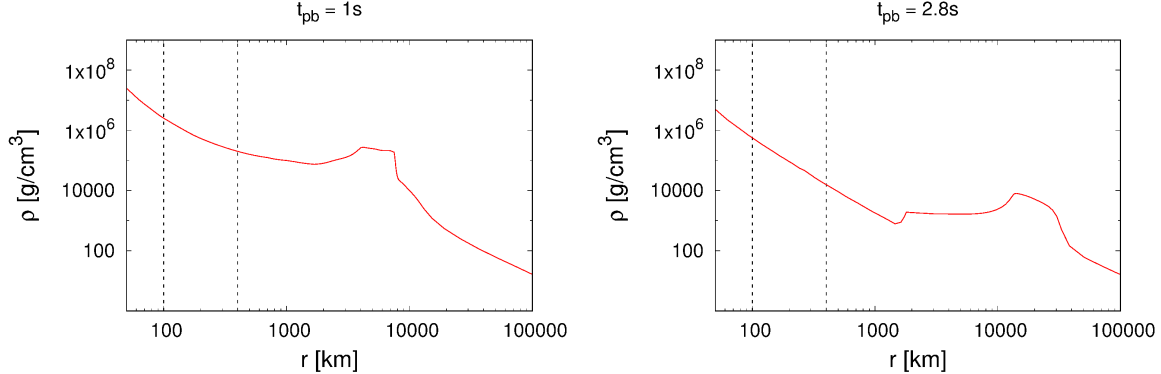


FIG. 2. The matter density profiles being used for the calculations of neutrino flavor transformation. The two dashed lines in each plot indicate the beginning and end of the calculation.

Thus we can add to the standard V-A self-interaction a new term given in equations (14) and/or (15) so that

$$H_{\text{SI}} = H_{\text{V-A}} + H_{\text{S/P}}. \quad (16)$$

At first glance the expressions for the NSSI looks very similar to the standard V-A term as both of them have a current-current nature. Where they differ in that wherever the V-A term uses the density matrix  $\rho_{\mathbf{p}}(\bar{\rho}_{\mathbf{p}}^*)$  the NSSI uses  $\rho_{\mathbf{p}}^*(\bar{\rho}_{\mathbf{p}})$ . In addition, the NSSI contains the matrices  $\tilde{\mathbf{g}}$  and/or  $\tilde{\mathbf{h}}$  which can include flavor-violating processes via their off-diagonal elements. As we shall see, these nuances are subtle but key for the NSSI to have observable effects when its overall strength is comparable to that of the standard V-A term. Since the contribution from scalar and pseudoscalar interactions have the same form we treat them as indistinguishable and focus on the phenomenological consequences of the scalar version of the NSSI.

We define two parameters  $\alpha_1$  and  $\alpha_2$  so that the  $\tilde{\mathbf{g}}$  matrix is parameterized as

$$\tilde{\mathbf{g}} = \left[ \frac{\sqrt{2}}{4} G_{\text{F}} \right]^{1/2} \begin{pmatrix} \alpha_1 & \alpha_2 & \alpha_2 \\ \alpha_2 & \alpha_1 & \alpha_2 \\ \alpha_2 & \alpha_2 & \alpha_1 \end{pmatrix}. \quad (17)$$

The  $\alpha_1$  indicates the strength of flavor-preserving (FP) NSSI while  $\alpha_2$  indicates the strength of flavor-violating (FV) NSSI. When the  $\alpha_1$  or  $\alpha_2$  is equal to unity it means the corresponding NSSI has an equal strength to the standard V-A interaction. For simplicity we have assumed the flavor-violating parameter is identical for all pairs between the 3 neutrino flavors but

Flavor	Luminosity $L_{\nu,\infty}$	Mean Energy $\langle E_{\nu,\infty} \rangle$	rms Energy $\sqrt{\langle E_{\nu,\infty}^2 \rangle}$
$e$	$4.606 \times 10^{51}$ erg/s	10.24 MeV	11.44 MeV
$\mu, \tau$	$5.473 \times 10^{51}$ erg/s	14.32 MeV	16.78 MeV
$\bar{e}$	$4.572 \times 10^{51}$ erg/s	12.88 MeV	14.51 MeV
$\bar{\mu}, \bar{\tau}$	$5.522 \times 10^{51}$ erg/s	14.42 MeV	16.93 MeV

TABLE I. The luminosities, mean energies, and rms energies used for the  $t_{pb} = 1.0$  s calculation.

note this is a restriction that can be relaxed. The neutrino mixing angles and square mass differences we adopt throughout the rest of the paper are  $m_2^2 - m_1^2 = 7.59 \times 10^{-5}$  eV<sup>2</sup>,  $|m_3^2 - m_2^2| = 2.32 \times 10^{-3}$  eV<sup>2</sup>  $\theta_{12} = 33.9^\circ$   $\theta_{13} = 9^\circ$  and  $\theta_{23} = 45^\circ$  which are consistent with the Particle Data Group evaluations [50]. The CP phase  $\delta_{\text{CP}}$  is set to zero. In the following calculations we will generally work with the inverted mass ordering (IMO) but will show some results using the normal mass ordering (NMO) and will indicate when this occurs.

The density profiles and neutrino spectra for our calculations comes from the 1-D GR-compatible CCSN simulation for the  $10.8 M_\odot$  progenitor calculated by Fischer *et al.* [51]. The matter density profiles are shown in figure (2). The neutrino emission is assumed to be half-isotropic and the neutrino spectra at  $r$  are given by the pinched thermal spectra found by Keil *et al.* [52]. Therefore we have

$$dn_\nu(r, \mathbf{p}) = \frac{L_{\nu,\infty}}{4\pi^2 R_\nu^2 \langle E_{\nu,\infty} \rangle} f_\nu(E) d(\cos\theta) d\phi \quad (18)$$

with

$$f_\nu(E) = \frac{(\gamma_\nu + 1)^{\gamma_\nu + 1}}{\Gamma(\gamma_\nu + 1)} \frac{E^{\gamma_\nu}}{\langle E_{\nu,\infty} \rangle^{\gamma_\nu + 1}} \exp\left(-\frac{(\gamma_\nu + 1)E}{\langle E_{\nu,\infty} \rangle}\right), \quad (19)$$

where  $\theta$  is the angle between the neutrino beams and the radial direction at  $r$ ,  $\phi$  the azimuthal angle of the beam,  $L_{\nu,\infty}$  the neutrino luminosity,  $\langle E_{\nu,\infty} \rangle$  the mean energy and  $\gamma_\nu$  the pinch parameter which can be derived from the mean energy  $\langle E_{\nu,\infty} \rangle$  and the mean square energy  $\langle E_{\nu,\infty}^2 \rangle$  via

$$\gamma_\nu = \frac{2\langle E_{\nu,\infty} \rangle^2 - \langle E_{\nu,\infty}^2 \rangle}{\langle E_{\nu,\infty}^2 \rangle - \langle E_{\nu,\infty} \rangle^2}. \quad (20)$$

The numerical values for the neutrino luminosities, mean and rms energies for post-bounce times of  $t_{pb} = 1.0$  s and  $t_{pb} = 2.8$  s are shown in tables (I) and (II). These two snapshots are representative of the early to intermediate cooling phase of CCSN explosion and were chosen based on the results from Wu *et al.* [53] which showed flavor transformations at

these two epochs for the  $18.0 M_{\odot}$  simulation by Fischer *et al.* [51] and the similarity of the neutrino spectra in this model with the  $10.8 M_{\odot}$  simulation also by Fischer *et al.* The neutrinosphere radius is set to  $R_{\nu} = 19$  km for the  $t_{pb} = 1.0$  s profile and  $R_{\nu} = 17$  km for the  $t_{pb} = 2.8$  s. For both time slices we compute the evolution starting from  $r = 100$  km. Our calculation adopts the multi-angle, multi-energy bulb model framework for energies ranging from 1 MeV to 60 MeV in 200 bins, and the neutrino emission angles ranging from  $0^{\circ}$  to  $90^{\circ}$  in 200 bins<sup>4</sup>. We have also verified our results have converged with the number of energy and angular bins.

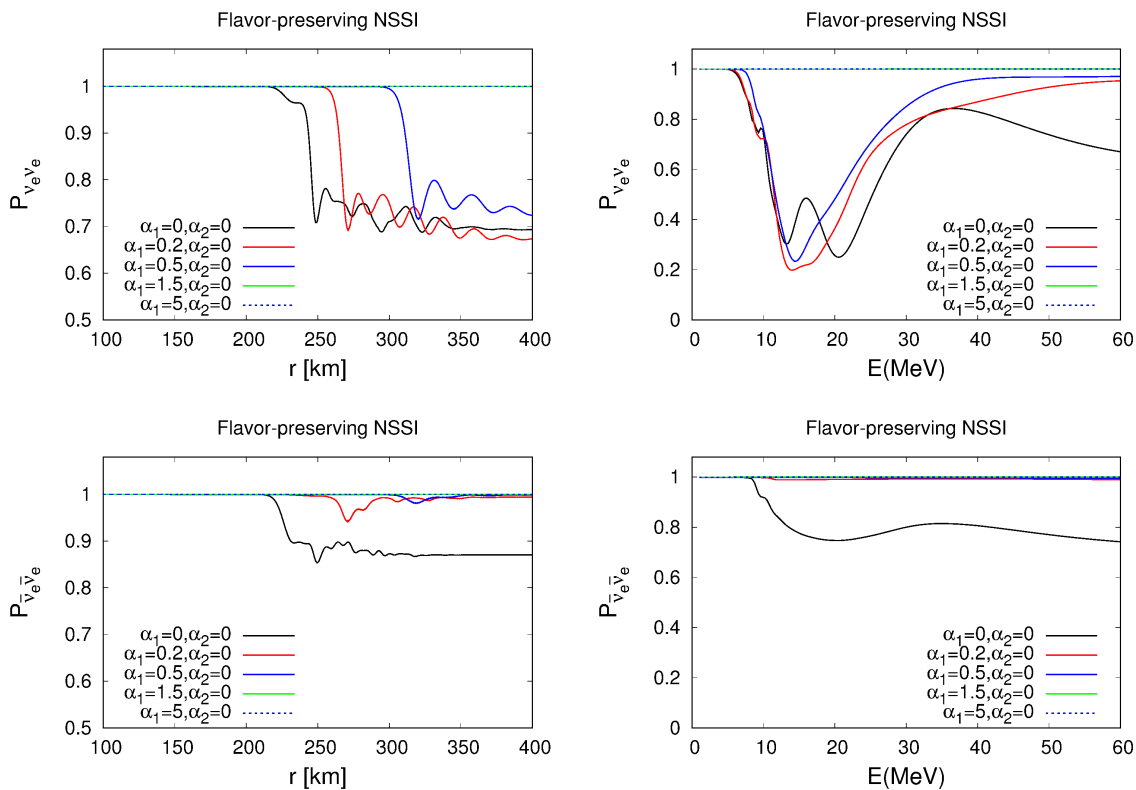


FIG. 3. Survival probability of electron neutrinos (top panels) and antineutrinos (bottom panels) with flavor-preserving NSSI at  $t_{pb} = 1.0s$ . The left panels are the flux averaged probabilities as a function of distance  $r$  while the right panels are plotted as function of energy at  $r = 400$  km. The combinations of the NSSI parameters are given in the legends.

<sup>4</sup> Determination of the number of angle bins needed in multi-angle calculations can be difficult. Insufficient angular resolution has been found to cause spurious flavor instabilities[54]. However, for the CCSN cooling phase, the matter density is generally not high enough for such artifacts to develop so the required number of angular bins can be reduced. Convergence has been checked to make sure 200 bins are sufficient for both  $t_{pb} = 1.0$  s and  $t_{pb} = 2.8$  s.

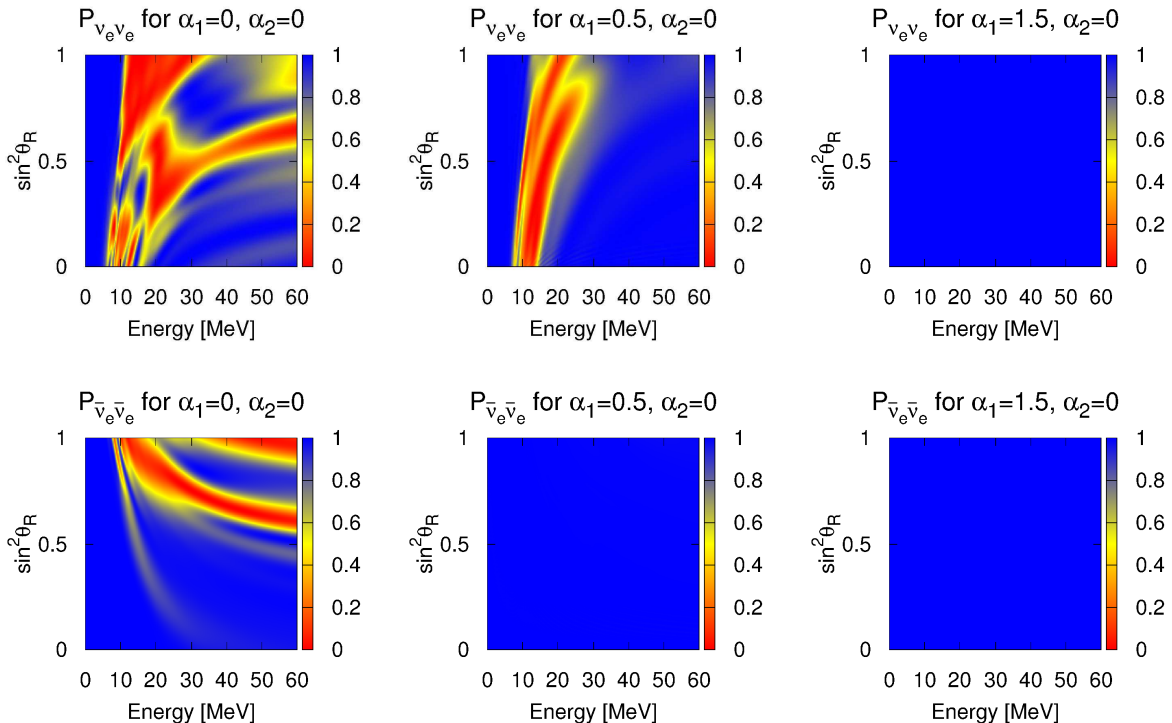


FIG. 4. Top panels: The heatmaps of survival probability of electron neutrinos at  $t_{pb} = 1.0s$  and  $r = 400km$  as a function of energy and emission angle when there is only flavor-preserving NSSI. Bottom panels: The same but for electron antineutrinos.

#### A. Flavor transformation at $t_{pb} = 1.0 s$

Figure (3) shows the numerical results of the survival probabilities of electron neutrino and antineutrino as a function of distance  $r$  from the neutrinosphere, for  $t_{pb} = 1.0 s$  and different values of  $\alpha_1$  when  $\alpha_2 = 0$ . In the left panels the probabilities are averaged over the energy and angular bins used in the calculation; in the right panels the survival probabilities are shown at  $r = 400 km$  as a function of neutrino energy averaged over the angular distribution only. we see that when there is no NSSI there is a noticeable amount of electron neutrinos transformation into muon and tau neutrinos, and that there are also flavor transformations in the electron antineutrino sector. This is in agreement with the results from Wu *et al.* [53]. When we add NSSI we can see the flavor transformation in neutrino sector is delayed although the average survival probability at  $r = 400 km$  is essentially unchanged. The spectra of the electron neutrinos at  $r = 400 km$  also look similar for the three values of  $\alpha_1$  shown though larger NSSI seems to suppress the transformation of the higher energy

neutrinos.

The flavor transformation in the antineutrino sector, however, is more affected by NSSI. As the NSSI is turned on, the transformation is immediately suppressed, with the final survival probability going back to  $P_{\bar{\nu}_e\bar{\nu}_e} = 1$ . This suppression effect can be seen more clearly in the sequence of 2-D plots shown figure (4), where we can see the region of flavor transformation keeps shrinking with an increasing NSSI in both neutrino and antineutrino sectors.

The effect of the NSSI becomes even more interesting when the flavor-violating NSSI parameter  $\alpha_2$  is non-zero. Figure 5 shows that the flavor-violating NSSI have the effect of undoing the suppression of the flavor-preserving NSSI. As we can see from the blue curve in the figure, the flavor transformation is restored to the original level (i.e. no NSSI) for the combination  $\alpha_1 = 1.5, \alpha_2 = 0.6$ . At smaller  $\alpha_2$ , the transformation is only partially restored across the spectrum, as shown by the red curve in the figure. The sequence of 2-D plots

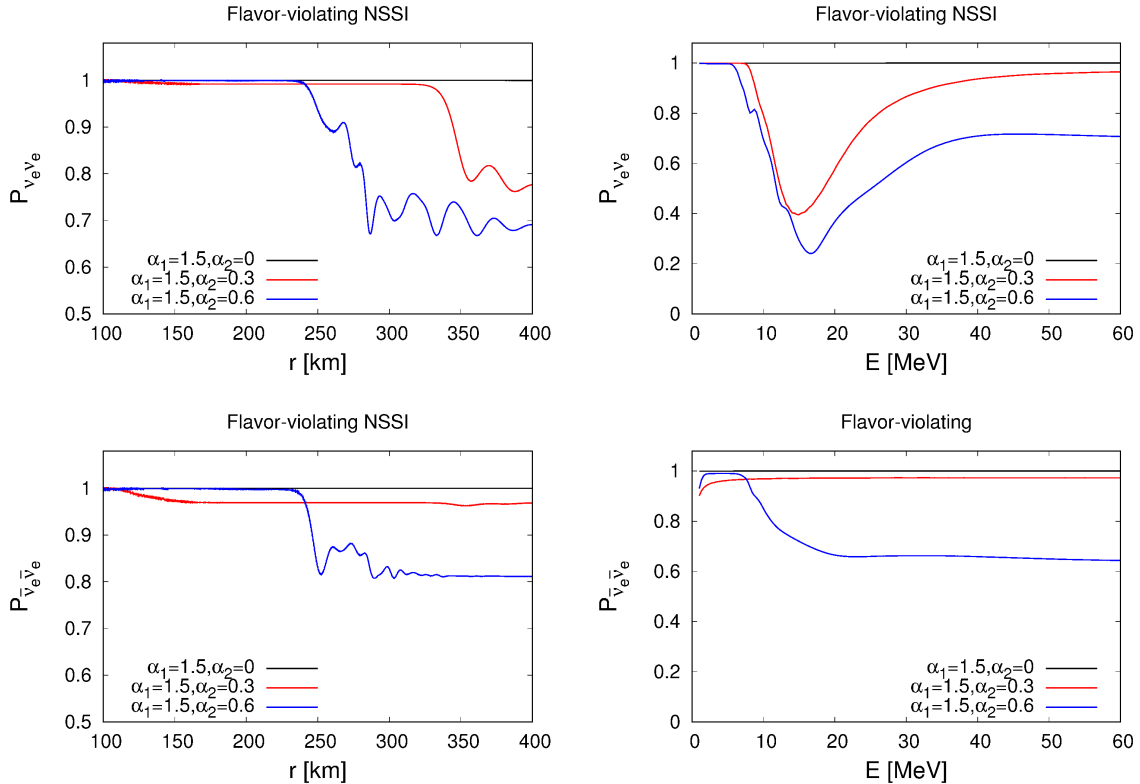


FIG. 5. Top panels: Survival probability of electron neutrinos at  $t_{pb} = 1.0s$  as a function of distance (left panel) and energy (right panel) at  $r = 400$  km with flavor-violating NSSI. The bottom panels are the same but for electron antineutrinos.

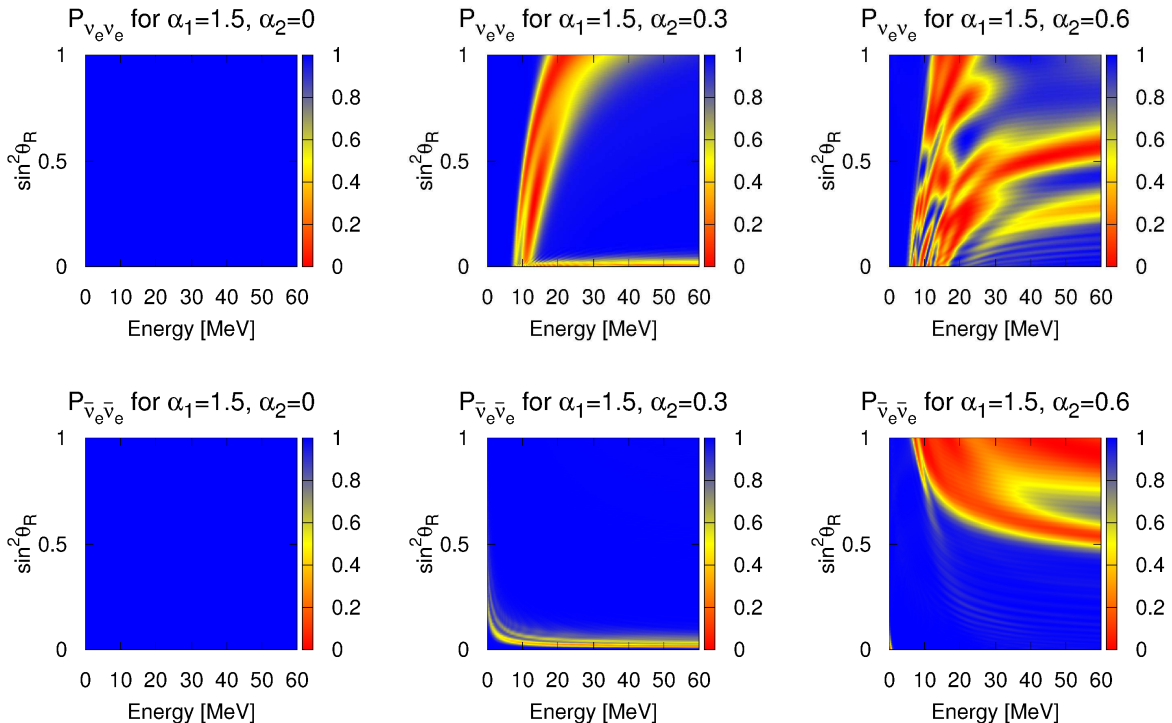


FIG. 6. Top panels: The heatmaps of survival probability of electron neutrinos at  $t_{pb} = 1.0s$  and  $r = 400km$  as a function of energy and emission angle when there is flavor-violating NSSI. Bottom panels: The same but for electron antineutrinos.

Flavor	Luminosity $L_{\nu, \infty}$	Mean Energy $\langle E_{\nu, \infty} \rangle$	rms Energy $\sqrt{\langle E_{\nu, \infty}^2 \rangle}$
$e$	$2.504 \times 10^{51}$ erg/s	9.891 MeV	11.12 MeV
$\mu, \tau$	$2.864 \times 10^{51}$ erg/s	12.66 MeV	14.99 MeV
$\bar{e}$	$2.277 \times 10^{51}$ erg/s	11.83 MeV	13.65 MeV
$\bar{\mu}, \bar{\tau}$	$2.875 \times 10^{51}$ erg/s	12.70 MeV	15.07 MeV

TABLE II. The luminosities, mean energies, and rms energies used for the  $t_{pb} = 2.8$  s calculation.

shown in figure 6 also show the pattern of transformed regions can be largely restored when flavor-violating NSSI is significant.

### B. Flavor transformation at $t_{pb} = 2.8$ s

In order to make sure the “shut-down” effect of NSSI is not specific to some certain settings of the supernova environment, we perform the same kind of calculations for the

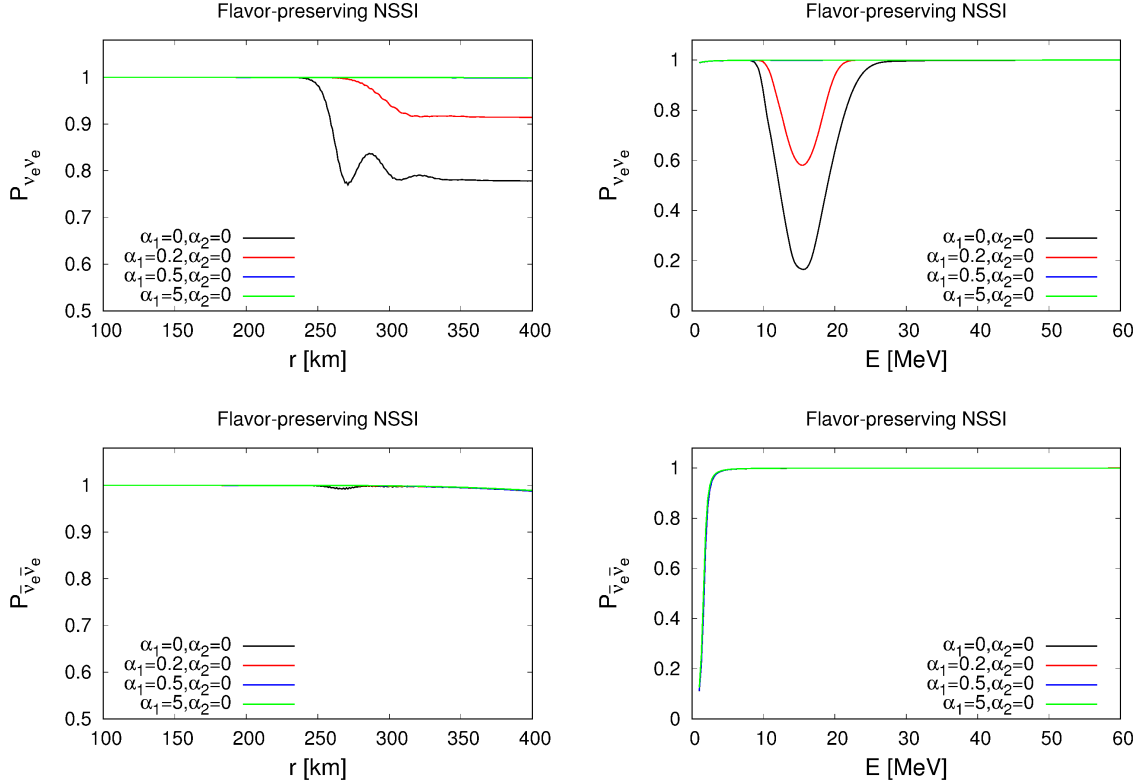


FIG. 7. Top panels: Survival probability of electron neutrinos at  $t_{pb} = 2.8$ s as a function of distance (left panel) and energy (right panel) at  $r = 400$  km with flavor-preserving NSSI. The bottom panels are the same but for electron antineutrinos.

$t_{pb} = 2.8$  s time slice of  $10.8 M_{\odot}$  progenitor. In figure (7) we plot the results with flavor-preserving NSSI only. It shows a similar “shut-down” effect in the neutrino sector as at  $t_{pb} = 1.0$  s. However, flavor transformation does not take place in the antineutrino sector with just the V-A term - this result is consistent with the Wu *et al.* results [53] - so there is no difference when NSSI is added. From the spectrum at  $r = 400$  km we can see the dip in the survival probability becomes shallower as NSSI increased, but the range of flavor transformation remains the same. The sequence of 2-D plots shown in figure (8) also show a shrinking of the transformed regions due to NSSI, similar to the shrinking seen in the  $t_{pb} = 1.0$  s case. And also as before, the effect of the flavor-violating NSSI is a restoration of flavor transformation to a state as if NSSI does not exist, as shown by figure (9) and (10).

Finally, it is also interesting to look at the effects of a pure flavor-violating NSSI. As seen in figure (11), the pure flavor-violating NSSI is capable of enforcing flavor transformation in the antineutrino sector for the IMO at the post-bounce time of  $t_{pb} = 2.8$  s, and the

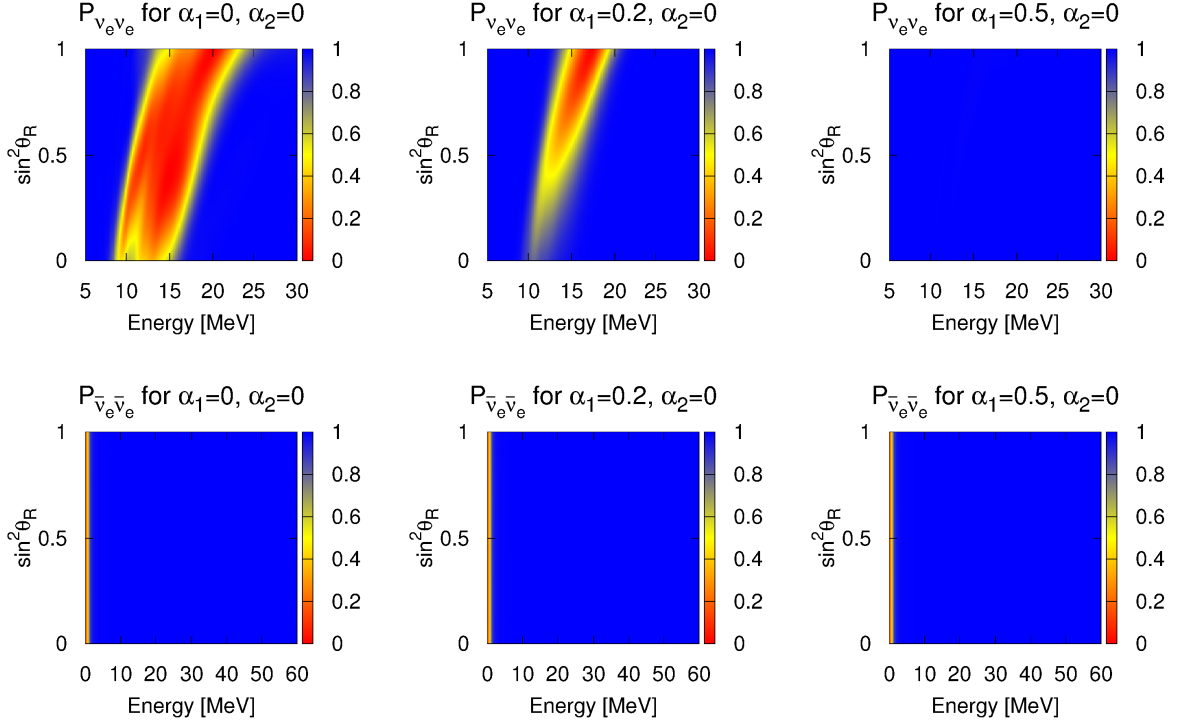


FIG. 8. Top panels: The heatmaps of survival probability of electron neutrinos at  $t_{pb} = 2.8s$  and  $r = 400km$  as a function of energy and emission angle when there is only flavor-preserving NSSI. Bottom panels: The same but for electron antineutrinos.

flavor transformation in the neutrino sector is also enhanced for this ordering. When the mass ordering is normal the NSSI can also lead to some flavor oscillations for both neutrino and antineutrinos, especially in the region close to the neutrinosphere, although the final survival probabilities are not very different from the result without NSSI even for the case where the flavor-violating parameter  $\alpha_2 = 2$ . These results for pure flavor-violating NSSI are qualitatively similar to that found by Das, Dighe and Sen with the gauge boson NSSI [34] but they are in contrast to those found for the IMO found in Wu *et al.* [53] who saw no transformation in the antineutrinos and only a small amount of transformation in the neutrinos at these late times using the 18.0  $M_\odot$  simulation by Fischer *et al.* [51] and computing the flavor transformation only using the standard V-A interaction.



### C. “Single-angle” vs “multi-angle” approach

In the previous sections we have demonstrated the suppression effect by flavor-preserving NSSI and the effect of undoing the suppression effect by the flavor-violating terms in the NSSI under the “multi-angle” framework. One often sees in the literature on supernova neutrinos reference to a “single-angle” approximation. This approximation assumes the evolution history of neutrinos is independent of its emission direction and is identical with that of the neutrinos propagating in a chosen direction<sup>5</sup>. This approximation has been used in previous works about NSSI and supernova neutrinos such as [27, 34]. The “single-angle” approximation greatly reduces runtimes but its drawback is that it has been known to produce collective flavor transformation which is not seen in “multi-angle” calculation

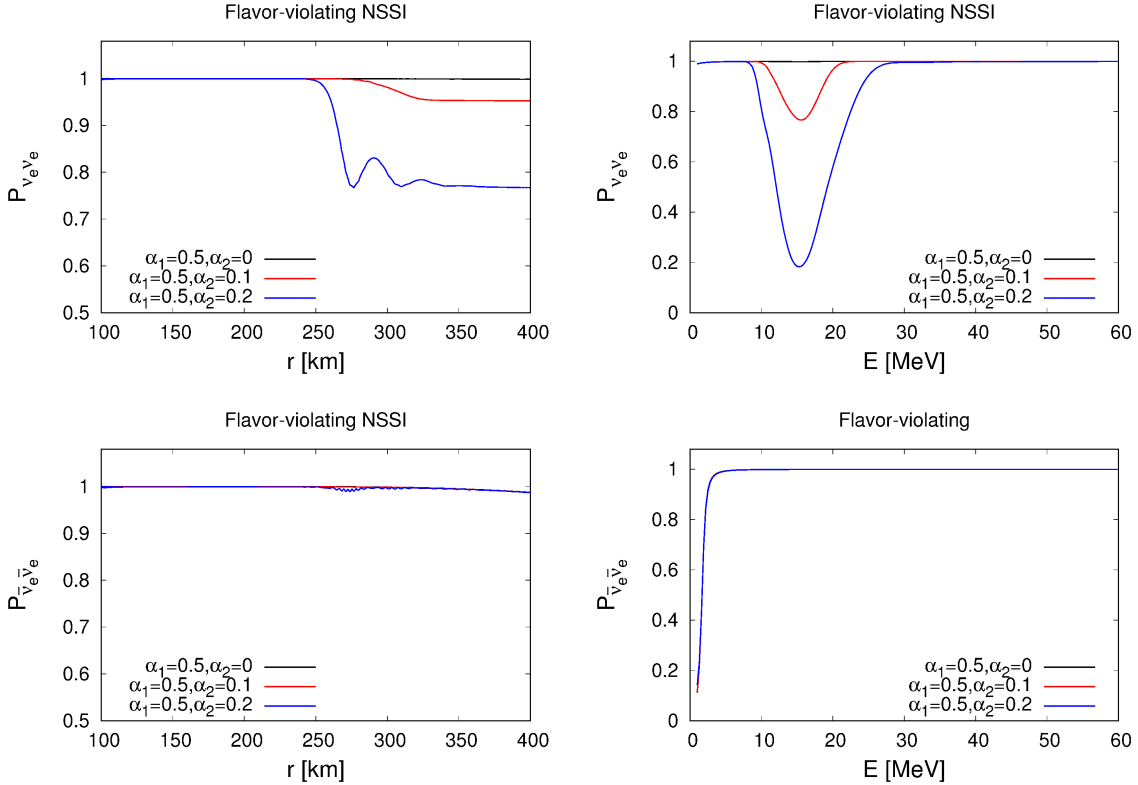


FIG. 9. Top panels: Survival probability of electron neutrinos at  $t_{pb} = 2.8s$  as a function of distance (left panel) and energy (right panel) at  $r = 400$  km with flavor-violating NSSI. Bottom panels: The same but for electron antineutrinos.

<sup>5</sup> The chosen direction is often set to be either the radial direction or  $45^\circ$  relative to the radial direction at the neutrinosphere. Here we adopted the radial direction.

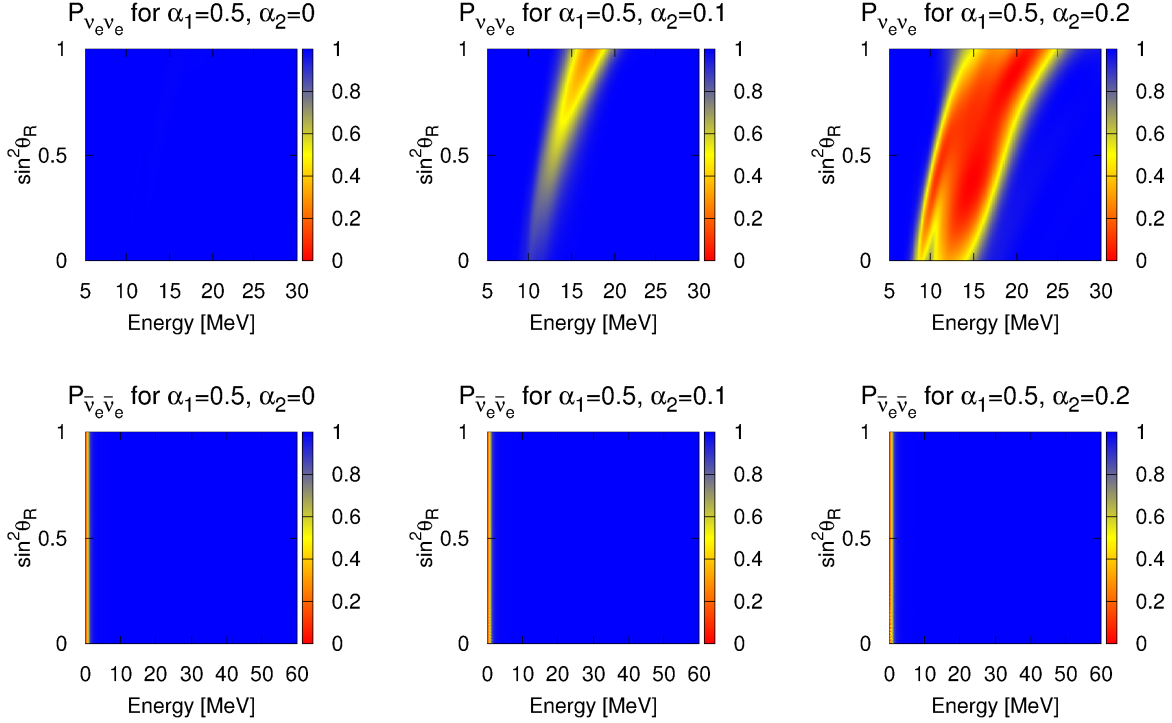


FIG. 10. Top panels: The heatmaps of survival probability of electron neutrinos at  $t_{pb} = 2.8s$  and  $r = 400km$  as a function of energy and emission angle when there is flavor-violating NSSI. Bottom panels: The same but for electron antineutrinos.

due to its artificial synchronization of different angular modes. While in some cases the “single-angle” approach gives qualitatively similar results as “multi-angle” approach, it also lacks the decoherence effect and can often result in flavor transformation occurring at much smaller radii than seen in multi-angle calculations [44]. In this section we compare the “multi-angle” results with “single-angle” counterparts to see whether the effects caused by NSSI can be reproduced more expediently in the single-angle calculations. In the “single-angle” approximation all neutrino with the same energy share the same evolution history regardless of their direction of propagation, so the NSSI Hamiltonian (14) and (15) can be simplified to be [5]

$$H_S(r) = \frac{D(r/R_\nu)}{2\pi R_\nu^2} \int \left\{ \tilde{\mathbf{g}} \left[ \rho^*(r, E) \frac{L_{\nu, \infty}}{\langle E_{\nu, \infty} \rangle} f_\nu(E) - \bar{\rho}(r, E) \frac{L_{\bar{\nu}, \infty}}{\langle E_{\bar{\nu}, \infty} \rangle} f_{\bar{\nu}}(E) \right] \tilde{\mathbf{g}} \right\} dE \quad (21)$$

$$H_P(r) = \frac{D(r/R_\nu)}{2\pi R_\nu^2} \int \left\{ \tilde{\mathbf{h}} \left[ \rho^*(r, E) \frac{L_{\nu, \infty}}{\langle E_{\nu, \infty} \rangle} f_\nu(E) - \bar{\rho}(r, E) \frac{L_{\bar{\nu}, \infty}}{\langle E_{\bar{\nu}, \infty} \rangle} f_{\bar{\nu}}(E) \right] \tilde{\mathbf{h}} \right\} dE \quad (22)$$

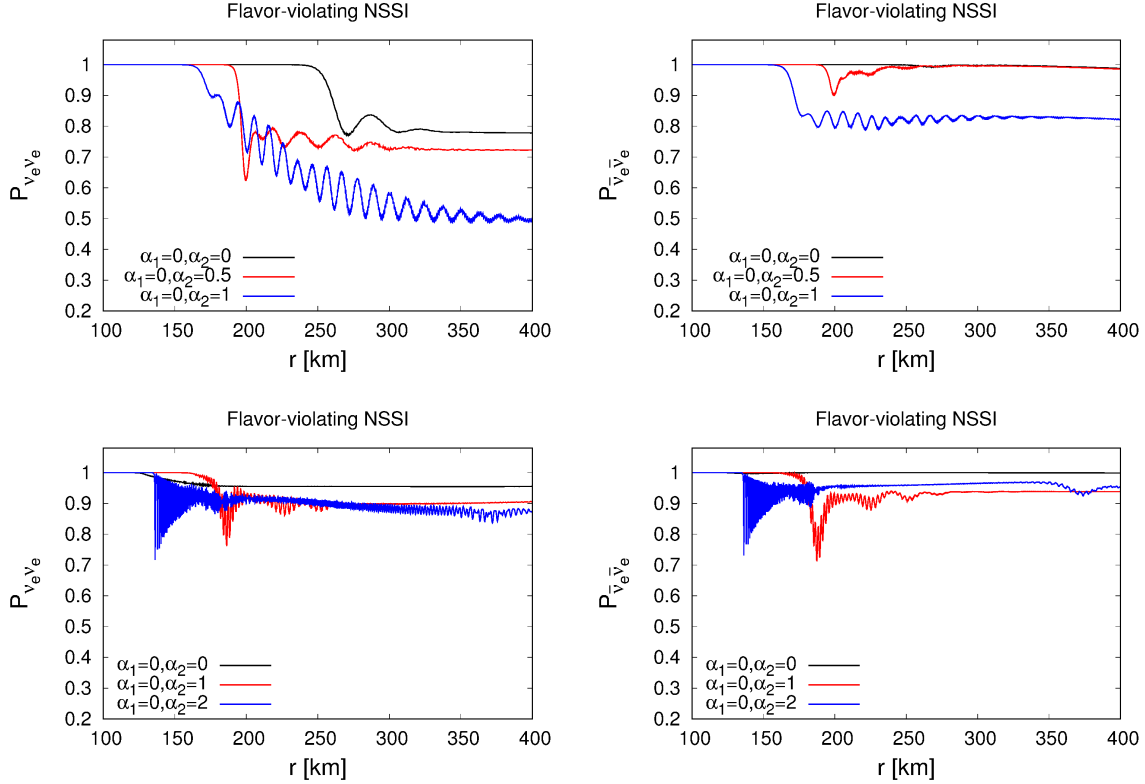


FIG. 11. Top panels: Survival probability of electron neutrinos and antineutrinos at  $t_{pb} = 2.8$ s as a function of distance with pure flavor violating NSI for IMO. Bottom panels: The same as top panels but for NMO.

where

$$D(r/R_\nu) = \frac{1}{2} \left[ 1 - \sqrt{1 - (R_\nu/r)^2} \right]^2 \quad (23)$$

is the geometric factor obtained after averaging over all the angular modes. The expression for the single-angle version of the V-A interactions can be found in Duan *et al.* [5].

In figure (12) we plot the survival probabilities for  $t_{pb} = 2.8$  s in neutrino sector computed with “single-angle” approach. In the upper panels, we only include the flavor-preserving NSI. Here we can see that unlike in the “multi-angle” case, the suppression effect is not as significant. In the final spectrum we notice that the NSI mostly affects the neutrinos from the high energy tail, which has a smaller weight in the overall ensemble. In the lower panels we again add the flavor-violating terms, and just as “multi-angle” case the effect of NSI is largely wiped out since the enhanced transformation in the high energy tail disappears. Thus it appears the presence of flavor-preserving NSI has different effects in “single-angle”

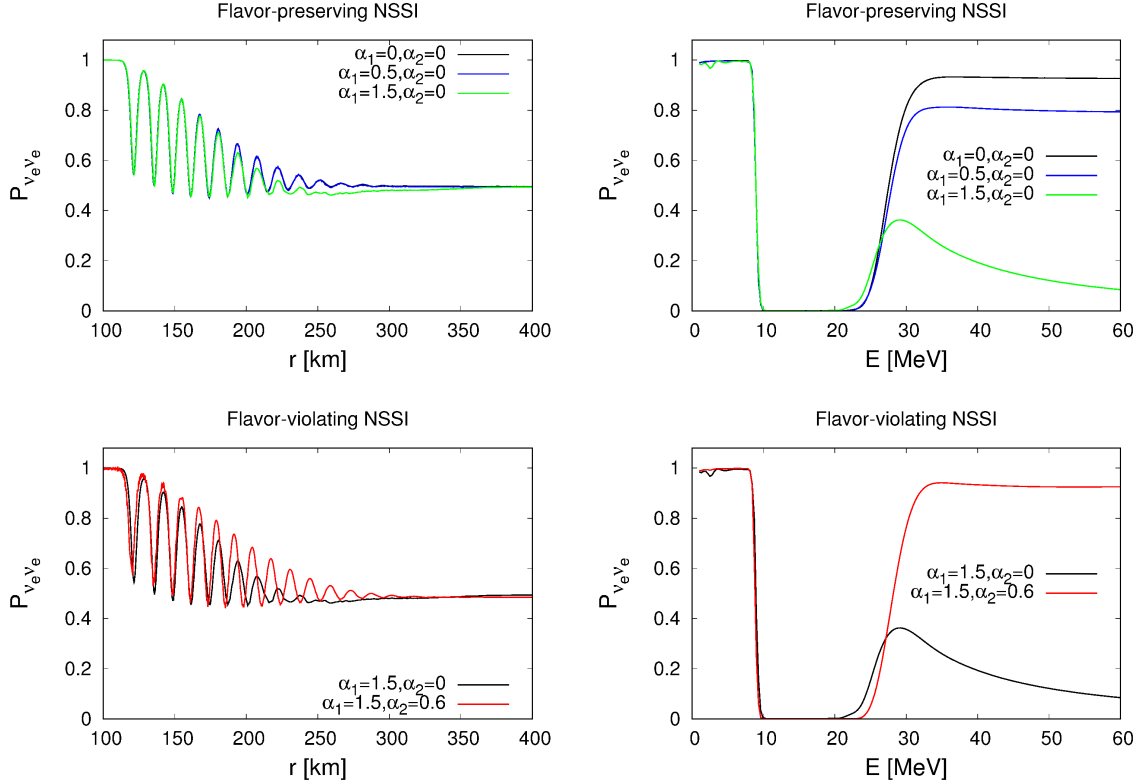


FIG. 12. Top panels: “Single-angle” survival probability of electron neutrinos at  $t_{pb} = 2.8$  s as a function of distance (left panel) and energy (right panel) at  $r = 400$  km with flavor-preserving NSSI. Bottom panels: The same but with flavor-violating terms.

and “multi-angle” cases but that single-angle does reproduce the correct trend that the flavor-violating terms always tends to undo any effect caused by flavor-preserving NSSI. The mechanism through which flavor-preserving NSSI shuts down collective oscillations in multi-angle calculation is still a point of interest that needs further investigation.

#### IV. SUMMARY AND DISCUSSION

In this paper we have derived the effective neutrino-neutrino Hamiltonian due to a NSSI with a scalar/pseudoscalar field and applied it to the case of neutrino flavor transformations at two epochs of a core-collapse supernova. We find that, as in the case of NSSI due to a new neutrino interaction via a gauge boson, there is a suppression effect of the flavor-preserving NSSI which is capable of delaying or shutting down entirely collective flavor oscillation when the strength of the NSSI is comparable to the standard V-A interaction. The presence of

flavor-violating terms in the NSSI has the effect of reducing the suppression effect of the flavor-preserving interactions and are capable of restoring the collective flavor oscillations to more-or-less the Standard Model behavior when sufficiently large. When flavor-violating interactions act along without flavor-preserving interactions, NSSI can increase flavor transformation over the V-A or induce oscillations in circumstances where the standard V-A does not. Finally, we find that while the single-angle approximation can give qualitatively similar results as we vary the NSSI parameters, there are large quantitative differences compared to multi-angle calculations.

The consideration of NSSI of supernova neutrinos provides many complimentary methods for the determination of neutrino properties. First, the effects of scalar or pseudoscalar NSSI could be useful as a complimentary method for identifying the Majorana or Dirac nature of the neutrino. Assuming the strength of the NSSI is of the order of the weak interaction, NSSI effects have nothing to do with the neutrino mass so appear even if the mass ordering is normal and the Majorana phases conspire to give an neutrinoless double beta decay effective Majorana mass  $m_{\beta\beta}$  which is exactly zero. At the same time, the presence or absence of NSSI signatures in the neutrino signal from a Galactic supernova neutrino burst provides a complimentary tool for measuring, or placing upper limits upon, the coupling strength of NSSI. Current bounds on neutrino-scalar coupling strength are given by a variety of analyses to be  $|g|^2 < 10^{-7} \sim 10^{-6}$  for scalar masses below 100 MeV, but there are presently no bounds for scalar masses above 300 MeV [55, 56]. The effective neutrino-neutrino self-interaction we derived is valid only for large scalar masses so NSSI of supernova neutrinos are able to provide constraints in what is currently a blank area in the neutrino-scalar exclusion plot. Finally, the NSSI we have considered in this paper are flavor neutral even though they may be flavor-violating. Other than simplicity, there is no reason to expect this to be true. The interaction strength might as well be unequal for different neutrino flavors or between different pairs of neutrino flavors, and that certainly would bring in new phenomenology, as indicated by the results from [34]. With their huge densities of neutrinos of all flavors, supernova environments provide an excellent laboratory for testing this assumption whatever the nature of the NSSI.

## ACKNOWLEDGEMENTS

The authors are grateful for many useful discussions with Gail McLaughlin and Alexey Vlasenko. This research is supported at NC State by the U.S. Department of Energy award DE-FG02-10ER41577.

### Appendix A: The mean field approximation

In this section we first derive the mean field expressions of the 4-neutrino operators, namely eq. (6) (7) (8) and (9). For generality we start by defining a generic 4-fermion operator as follows

$$M_{1234}^{ab} = (\bar{\psi}_1 \Gamma^a \psi_2) (\bar{\psi}_3 \Gamma^b \psi_4), \quad (\text{A1})$$

here  $\Gamma^a$  can be anyone of the 16  $\Gamma$ -matrices forming the basis of the vectorial space of all  $4 \times 4$  matrices. Applying the mean field approximation on the 4-fermion operator results in the following expression

$$\begin{aligned} M_{1234}^{ab} \approx & \langle \bar{\psi}_1 \Gamma^a \psi_2 \rangle (\bar{\psi}_3 \Gamma^b \psi_4) + \langle \bar{\psi}_3 \Gamma^b \psi_4 \rangle (\bar{\psi}_1 \Gamma^a \psi_2) - \\ & \sum_{c,d=S,P,V,A,T} C_{ab,cd} \left[ \langle \bar{\psi}_3 \Gamma^d \psi_2 \rangle (\bar{\psi}_1 \Gamma^c \psi_4) + \langle \bar{\psi}_1 \Gamma^c \psi_4 \rangle (\bar{\psi}_3 \Gamma^d \psi_2) \right]. \end{aligned} \quad (\text{A2})$$

The first two terms of equation (A2) represent the regular ‘‘Hartree terms’’, while the following terms inside the summation are the ‘‘exchange terms’’ arising from the mean field treatment [57]. Note that: a *Fierz transformation* has been performed to the ‘‘exchange terms’’ since the fermion operators contain spinors, we have dropped the constant term that is present in the mean field expression because it does not have any effect in the evolution equations. In the case of scalar-scalar interaction, we have  $a, b = S$ . Replacing the generic fermion fields  $\psi$  with neutrino fields, we have

$$\begin{aligned} (\bar{\nu}_1 \nu_2) (\bar{\nu}_3 \nu_4) \approx & \langle \bar{\nu}_1 \nu_2 \rangle (\bar{\nu}_3 \nu_4) + \langle \bar{\nu}_3 \nu_4 \rangle (\bar{\nu}_1 \nu_2) - \\ & \sum_{c,d=S,P,V,A,T} C_{SS,cd} \left[ \langle \bar{\nu}_3 \Gamma^d \nu_2 \rangle (\bar{\nu}_1 \Gamma^c \nu_4) + \langle \bar{\nu}_1 \Gamma^c \nu_4 \rangle (\bar{\nu}_3 \Gamma^d \nu_2) \right]. \end{aligned} \quad (\text{A3})$$

In the relativistic limit only vector and pseudovector terms can survive the averaging in the single-particle state [58] so we can drop all terms in the right-hand side of equation (A3)

except for the terms with  $V \times V$  or  $A \times A$  form. Therefore we are left with

$$\begin{aligned} (\bar{\nu}_1 \nu_2) (\bar{\nu}_3 \nu_4) &\approx -\frac{1}{4} \langle \bar{\nu}_1 \Gamma^V \nu_4 \rangle (\bar{\nu}_3 \Gamma^V \nu_2) + \frac{1}{4} \langle \bar{\nu}_1 \Gamma^A \nu_4 \rangle (\bar{\nu}_3 \Gamma^A \nu_2) + (14 \leftrightarrow 32) \\ &= -\frac{1}{2} \langle \bar{\nu}_1 \gamma^\mu P_R \nu_4 \rangle (\bar{\nu}_3 \gamma^\mu P_L \nu_2) - \frac{1}{2} \langle \bar{\nu}_1 \gamma^\mu P_L \nu_4 \rangle (\bar{\nu}_3 \gamma^\mu P_R \nu_2) + (14 \leftrightarrow 32), \end{aligned} \quad (\text{A4})$$

where  $\Gamma^V \equiv \gamma^\mu$ ,  $\Gamma^A \equiv \gamma^\mu \gamma^5$  and  $P_{L/R} = \frac{1}{2}(1 \mp \gamma^5)$  are the projection operators. Decomposing the neutrino into  $\nu = \begin{pmatrix} \nu_L & \nu_R \end{pmatrix}^T$  for Dirac neutrinos, and  $\nu = \begin{pmatrix} \nu_L & \nu_L^C \end{pmatrix}^T$  for Majorana neutrino, we eventually obtain equations (6) and (8). The derivation for the equations (7) and (9) follows a similar path.

Next we derive the expressions for equations (11) and (12). First we write down the quantized field operator for Majorana neutrino

$$\nu(x) = \sum_{h=\pm 1} \sum_p \frac{1}{2EV} \left[ a^{(h)}(p) u^{(h)}(p) e^{-ip \cdot x} + a^{(h)\dagger}(p) v^{(h)}(p) e^{ip \cdot x} \right] \equiv \nu^C(x), \quad (\text{A5})$$

where  $x \equiv x^\mu$  is the 4-position and  $p \equiv p^\mu$  is the 4-momentum. Then we can decompose the neutrino field into its 2 chirality components  $\nu_L(x) = P_L \nu(x)$  and  $\nu_L^C(x) = P_R \nu(x)$ . If neutrino has mass then both helicity states are present for each of the 2 chirality fields. But in the relativistic limit, for each helicity state, one of the 2 chirality components will be suppressed, resulting in the following equations

$$\nu_L(x) = \sum_p \frac{1}{2EV} \left[ a^{(-)}(p) u^{(-)}(p) e^{-ip \cdot x} + a^{(+)\dagger}(p) v^{(+)}(p) e^{ip \cdot x} \right], \quad (\text{A6})$$

and

$$\nu_L^C(x) = \sum_p \frac{1}{2EV} \left[ a^{(+)}(p) u^{(+)}(p) e^{-ip \cdot x} + a^{(-)\dagger}(p) v^{(-)}(p) e^{ip \cdot x} \right], \quad (\text{A7})$$

Since Majorana particles are their own antiparticles, we cannot distinguish a Majorana neutrino from an antineutrino by their creation and annihilation operators. Nevertheless it is customary to call Majorana neutrino with negative(positive) helicity *neutrino(antineutrino)*, therefore we have (flavor subscripts omitted)

$$|\nu(\mathbf{p})\rangle \equiv |\nu(p)\rangle = \frac{1}{\sqrt{2EV}} a^{(-)\dagger}(p) |0\rangle, \quad |\bar{\nu}(\mathbf{p})\rangle \equiv |\bar{\nu}(p)\rangle = \frac{1}{\sqrt{2EV}} a^{(+)\dagger}(p) |0\rangle, \quad (\text{A8})$$

Note we adopt the finite volume normalization convention from [59] so that the 4-momentum is summed instead of integrated. The corresponding commutation relations for the creation and annihilation operators are

$$\left\{ a_\alpha^{(h)}(p), a_\beta^{(h')\dagger}(p') \right\} = (2EV) \delta_{\alpha\beta} \delta_{hh'} \delta_{pp'}, \quad (\text{A9})$$

with  $\alpha, \beta$  denoting the neutrino flavor. Combining equations (A6), (A7), (A8) and (A9), we can obtain the current equations (11) and (12) with the flavor-superposition states (10).

- 
- [1] G. Sigl and G. Raffelt, Nuclear Physics B **406**, 423 (1993).
  - [2] P. Strack and A. Burrows, Phys. Rev. D **71**, 093004 (2005), hep-ph/0504035.
  - [3] C. Volpe, D. Väänänen, and C. Espinoza, Phys. Rev. D **87**, 113010 (2013), arXiv:1302.2374 [hep-ph].
  - [4] A. Vlasenko, G. M. Fuller, and V. Cirigliano, Phys. Rev. D **89**, 105004 (2014), arXiv:1309.2628 [hep-ph].
  - [5] H. Duan, G. M. Fuller, J. Carlson, and Y.-Z. Qian, Phys. Rev. D **74**, 105014 (2006), arXiv:astro-ph/0606616 [astro-ph].
  - [6] S. Horiuchi and J. P. Kneller, ArXiv e-prints (2017), arXiv:1709.01515 [astro-ph.HE].
  - [7] A. Mirizzi, I. Tamborra, H.-T. Janka, N. Saviano, K. Scholberg, R. Bollig, L. Hüdepohl, and S. Chakraborty, Nuovo Cimento Rivista Serie **39**, 1 (2016), arXiv:1508.00785 [astro-ph.HE].
  - [8] H. Nunokawa, J. T. Peltoniemi, A. Rossi, and J. W. F. Valle, Phys. Rev. D **56**, 1704 (1997), hep-ph/9702372.
  - [9] G. C. McLaughlin, J. M. Fetter, A. B. Balantekin, and G. M. Fuller, Phys. Rev. C **59**, 2873 (1999), astro-ph/9902106.
  - [10] O. L. G. Peres and A. Y. Smirnov, Nuclear Physics B **599**, 3 (2001), hep-ph/0011054.
  - [11] J. Beun, G. C. McLaughlin, R. Surman, and W. R. Hix, Phys. Rev. D **73**, 093007 (2006), hep-ph/0602012.
  - [12] I. Tamborra, G. G. Raffelt, L. Hüdepohl, and H.-T. Janka, JCAP **1201**, 013 (2012), arXiv:1110.2104 [astro-ph.SR].
  - [13] M. L. Warren, M. Meixner, G. Mathews, J. Hidaka, and T. Kajino, Phys. Rev. D **90**, 103007 (2014), arXiv:1405.6101 [astro-ph.HE].
  - [14] M.-R. Wu, T. Fischer, L. Huther, G. Martínez-Pinedo, and Y.-Z. Qian, Phys. Rev. D **89**, 061303 (2014), arXiv:1305.2382 [astro-ph.HE].
  - [15] A. Esmaili, O. L. G. Peres, and P. D. Serpico, Phys. Rev. D **90**, 033013 (2014), arXiv:1402.1453 [hep-ph].
  - [16] S. P. Mikheyev and A. Y. Smirnov, Yad. Fiz. **42**, 1441 (1985), (*Sov. J. Nucl. Phys.* **42** 913).



- [17] S. P. Mikheyev and A. Y. Smirnov, in *'86 Massive Neutrinos in Astrophysics and in Particle Physics*, edited by O. Frackler and J. Trân Thanh Vân (Editions Frontières, Gif-sur-Yvette, 1986) p. 355.
- [18] L. Wolfenstein, *Phys. Rev. D* **17**, 2369 (1978).
- [19] O. G. Miranda and H. Nunokawa, *New Journal of Physics* **17**, 095002 (2015).
- [20] T. Ohlsson, *Reports on Progress in Physics* **76**, 044201 (2013), arXiv:1209.2710 [hep-ph].
- [21] J. W. F. Valle, *Physics Letters B* **199**, 432 (1987).
- [22] H. Nunokawa, Y.-Z. Qian, A. Rossi, and J. W. F. Valle, *Phys. Rev. D* **54**, 4356 (1996), hep-ph/9605301.
- [23] H. Nunokawa, A. Rossi, and J. W. F. Valle, *Nuclear Physics B* **482**, 481 (1996), hep-ph/9606445.
- [24] S. W. Mansour and T. K. Kuo, *Phys. Rev. D* **58**, 013012 (1998), hep-ph/9711424.
- [25] G. L. Fogli, E. Lisi, A. Mirizzi, and D. Montanino, *Phys. Rev. D* **66**, 013009 (2002), hep-ph/0202269.
- [26] A. Esteban-Pretel, R. Tomàs, and J. W. F. Valle, *Phys. Rev. D* **76**, 053001 (2007).
- [27] M. Blennow, A. Mirizzi, and P. D. Serpico, *Phys. Rev. D* **78**, 113004 (2008), arXiv:0810.2297 [hep-ph].
- [28] A. Esteban-Pretel, R. Tomàs, and J. W. F. Valle, *Phys. Rev. D* **81**, 063003 (2010), arXiv:0909.2196 [hep-ph].
- [29] C. J. Stapleford, D. J. Väänänen, J. P. Kneller, G. C. McLaughlin, and B. T. Shapiro, *Phys. Rev. D* **94**, 093007 (2016), arXiv:1605.04903 [hep-ph].
- [30] M. S. Bilenky, S. M. Bilenky, and A. Santamaria, *Phys. Lett. B* **301**, 287 (1993).
- [31] M. S. Bilenky and A. Santamaria, *Phys. Lett. B* **336**, 91 (1994), arXiv:hep-ph/9405427 [hep-ph].
- [32] E. Masso and R. Toldra, *Phys. Lett. B* **333**, 132 (1994), arXiv:hep-ph/9404339 [hep-ph].
- [33] M. S. Bilenky and A. Santamaria, in *Neutrino mixing. Festschrift in honour of Samoil Bilenky's 70th birthday. Proceedings, International Meeting, Turin, Italy, March 25-27, 1999* (1999) pp. 50–61, arXiv:hep-ph/9908272 [hep-ph].
- [34] A. Das, A. Dighe, and M. Sen, *JCAP* **1705**, 051 (2017), arXiv:1705.00468 [hep-ph].
- [35] G. B. Gelmini and M. Roncadelli, *Phys. Lett. B* **99**, 411 (1981).
- [36] G. B. Gelmini, S. Nussinov, and M. Roncadelli, *Nucl. Phys. B* **209**, 157 (1982).

- [37] E. W. Kolb and M. S. Turner, *Phys. Rev.* **D 36**, 2895 (1987).
- [38] S. Chang and K. Choi, *Phys. Rev.* **D 49**, 12 (1994), arXiv:hep-ph/9303243 [hep-ph].
- [39] K. Choi, C. W. Kim, J. Kim, and W. P. Lam, *3rd Asia Pacific Physics Conference Hong Kong, June 20-24, 1988*, *Phys. Rev.* **D 37**, 3225 (1988).
- [40] M. Kachelriess, R. Tomas, and J. W. F. Valle, *Phys. Rev.* **D 62**, 023004 (2000), arXiv:hep-ph/0001039 [hep-ph].
- [41] R. Tomas, H. Pas, and J. W. F. Valle, *Phys. Rev.* **D 64**, 095005 (2001), arXiv:hep-ph/0103017 [hep-ph].
- [42] Y. Farzan, *Phys. Rev.* **D 67**, 073015 (2003), arXiv:hep-ph/0211375 [hep-ph].
- [43] S. Chakraborty, T. Fischer, A. Mirizzi, N. Saviano, and R. Tomàs, *Phys. Rev. Lett.* **107**, 151101 (2011), arXiv:1104.4031 [hep-ph].
- [44] H. Duan and A. Friedland, *Phys. Rev. Lett.* **106**, 091101 (2011), arXiv:1006.2359 [hep-ph].
- [45] R. F. Sawyer, *Phys. Rev. D* **72**, 045003 (2005), hep-ph/0503013.
- [46] A. Mirizzi and P. D. Serpico, *Phys. Rev. Lett.* **108**, 231102 (2012), arXiv:1110.0022 [hep-ph].
- [47] N. Saviano, S. Chakraborty, T. Fischer, and A. Mirizzi, *Phys. Rev. D* **85**, 113002 (2012), arXiv:1203.1484 [hep-ph].
- [48] B. Dasgupta, A. Mirizzi, and M. Sen, *JCAP* **2**, 019 (2017), arXiv:1609.00528 [hep-ph].
- [49] Y. Yang and J. P. Kneller, *Phys. Rev.* **D96**, 023009 (2017), arXiv:1705.09723 [astro-ph.HE].
- [50] C. Patrignani *et al.* (Particle Data Group), *Chin. Phys.* **C40**, 100001 (2016).
- [51] T. Fischer, S. C. Whitehouse, A. Mezzacappa, F. K. Thielemann, and M. Liebendorfer, *Astron. Astrophys.* **517**, A80 (2010), arXiv:0908.1871 [astro-ph.HE].
- [52] M. T. Keil, G. G. Raffelt, and H.-T. Janka, *Astrophys. J.* **590**, 971 (2003), astro-ph/0208035.
- [53] M.-R. Wu, Y.-Z. Qian, G. Martínez-Pinedo, T. Fischer, and L. Huther, *Phys. Rev. D* **91**, 065016 (2015).
- [54] S. Sarikas, D. de Sousa Seixas, and G. Raffelt, *Physical Review D* **86**, 125020 (2012).
- [55] P. S. Pasquini and O. L. G. Peres, *Phys. Rev.* **D 93**, 053007 (2016), [Erratum: *Phys. Rev. D* **93**, no.7, 079902 (2016)], arXiv:1511.01811 [hep-ph].
- [56] L. Heurtier and Y. Zhang, *JCAP* **1702**, 042 (2017), arXiv:1609.05882 [hep-ph].
- [57] H. Bruus and K. Flensberg, *Many-body quantum theory in condensed matter physics: an introduction* (Oxford University Press, 2004) pp. 69–71.
- [58] S. Bergmann, Y. Grossman, and E. Nardi, *Phys. Rev.* **D 60**, 093008 (1999),

arXiv:hep-ph/9903517 [hep-ph].

- [59] C. Giunti and K. C. Wook, *Fundamentals of Neutrino Physics and Astrophysics* (Oxford Univ., Oxford, 2007).